Development of CdTe detectors in Acrorad

Minoru Funaki, Yukio Ando, Ryuji Jinnai, Akira Tachibana and Ryoichi Ohno
Acrorad Co., Ltd.
e-mail: funaki@acrorad.jp

1. Introduction

Thanks to the high resistivity at room temperature and the large linear attenuation coefficient, CdTe became to be considered a prospective material for the room temperature semiconductor detector in 1970s [1~3]. The growth technologies of CdTe single crystal by Traveling Heater Method (THM) as well as the detector fabrication process have been intensively developed for almost 2 decades [4~10] in Acrorad Co., Ltd.

In this workshop, the growth of CdTe single crystal by THM and the characteristics of CdTe detectors are presented with some medical applications.

2. CdTe single crystal growth by THM

The Cd-Te phase diagram is shown in Fig.1 [11]. This phase diagram shows that CdTe can be crystallized from the Te-rich Cd-Te solution at much lower temperature than the melting temperature of stoichiometric CdTe (1092 °C), so that the impurity contamination from the quartz ampoule is suppressed during the growth.

Fig.2 shows the schematic diagram of the THM growth. A CdTe single crystal seed, Te-rich alloy and the CdTe poly-crystal rod are charged into the quartz ampoule, which is later sealed with inert gas. The $CdCl_2$ is added to the Te-rich alloy for Cl doping to maximize the resistivity and the carrier lifetime [5,7,9]. By heating up the furnace, only the Te-rich alloy melts and the molten zone is formed. As the temperature of the lower end of the CdTe poly-crystal rod increases by moving down the ampoule slowly, the solubility of CdTe increases and the CdTe poly crystal is dissolved into the molten zone. At the same time, the temperature of the upper surface of the CdTe seed decreases, CdTe is crystallized from the molten zone onto the seed. Finally, the whole CdTe poly crystal rod is dissolved and re-crystallized on the CdTe seed by the travel of the ampoule in the whole length.

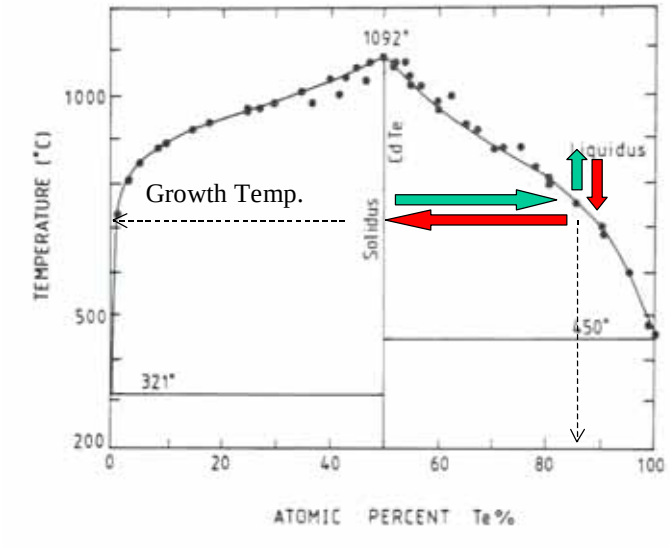

Figure 1 The Cd-Te phase diagram [11]

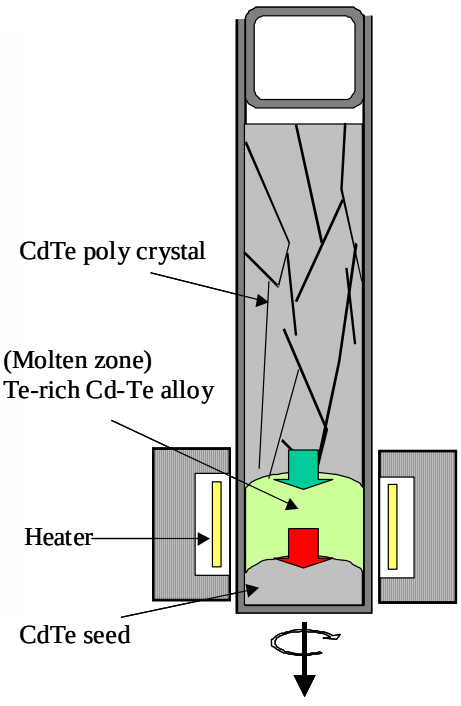

Fig.2 The schematic diagram of CdTe THM growth

Shown in Fig.3 are the CdTe single crystals grown at Acrorad. The development of the THM crystal growth started in 1988, the crystal size was 32mm in diameter, 120mm in length and 560g in weight. Now the CdTe single crystal of 75mm in diameter, 220mm in length, 5680g in weight is regularly grown. The weight of the crystal ingot became 10 times comparing to the first generation. The single crystal yield was 87% in 2006.

Fig.4 is the photograph of the single crystal wafers cut from the crystal ingot of 75mm diameter. The rectangular shaped wafers were sliced with (111) orientation and the size is larger than 50 x 50 mm^2. Thanks to the scale up of the CdTe ingot (wafer) and the increase of the single crystal yield, the large area detector (e.g. 25 x 25 mm^2) can be regularly fabricated mainly for the imaging applications.

Fig. 3 The CdTe single crystals grown at Acrorad

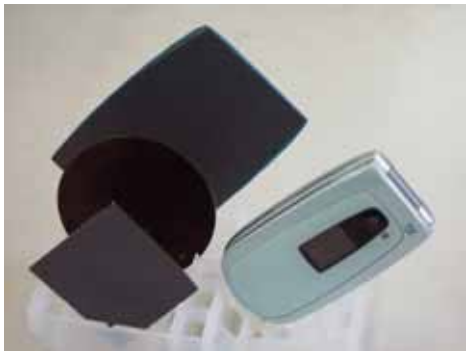

Fig.4 Single crystal wafers

3. Characteristics of CdTe detectors

Two types of the detector, "Ohmic detector"[4] and "Schottky detector" [12,13] have been fabricated in Acrorad. The wafer is mechano-chemically polished followed by the electrode deposition. The "Ohmic detector" has platinum contacts on both surfaces, while the "Schottky detector" has an indium–titanium multi-layer contact and a platinum contact, as seen in Fig.5. The platinum contact is fabricated by the electroless plating, while the indium and titanium contact are formed by the vacuum evaporation [8,10].

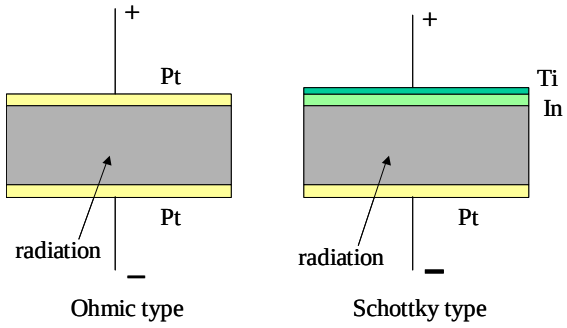

Fig.5 The structure of the "Ohmic detector" and the "Schottky detector"

Fig.6 (left) shows the I-V characteristics of the "Ohmic detector" (size: 4 x 4 x 1mm^3) at 25°C. The I-V is not a straight line probably due to the space charge limited current [5]. The dark current at bias 70V, which is the optimum bias to obtain the best energy spectrum, is 70nA, so the detector resistivity is 1.8 x10^9 Ωcm.

The I-V of the "Schottky detector" is shown Fig.6 (right). Due to the indium Schottky contact, the injection of the hole is suppressed and the dark current is very small comparing to "Ohmic detector" when the indium contact is anode. The dark current at 700V (optimum for the energy spectrum) is only 3nA, so the resistivity of the detector is 3.7 x 10^{11} Ωcm. This is higher than that of the "Ohmic detector" by two orders.

Fig.7 shows the typical energy spectra of the "Ohmic detector" and the " Schottky detector" of 4 x 4 x 1mm^3 at 25°C. The applied bias voltage was optimized for the best energy resolution, i.e. 60V for ^{241}Am and ^{57}Co and 100V for ^{137}Cs, while that for the "Schottky detector" was 700V for all gamma ray sources.

The "Ohmic detector" shows the moderate energy resolution with some tails to the low energy side of the photo-peaks, clearly indicating that some carriers are trapped in the detector. On the other hand, the FWHM of the "Schottky detector" is almost half of the "Ohmic detector", due to the one order higher electric field and one order smaller dark current. As the high electric field reduce the charge collection time, it would be probably more suitable for the PET application with the better time resolution.

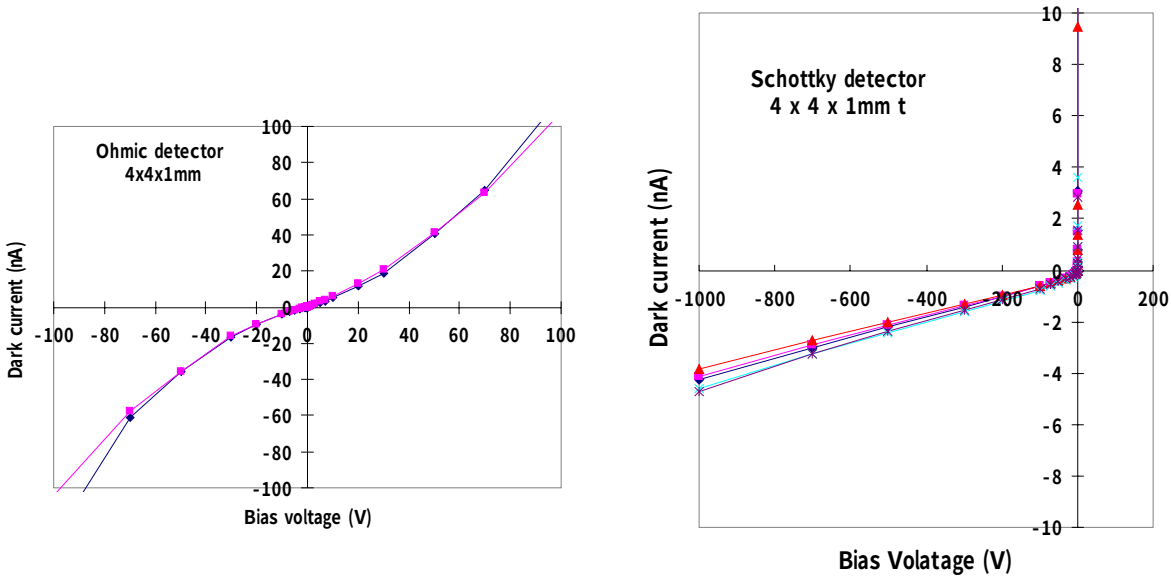

Fig.6 I-V curves of the “Ohmic detector”(left) and the “Schottky detector” (right)

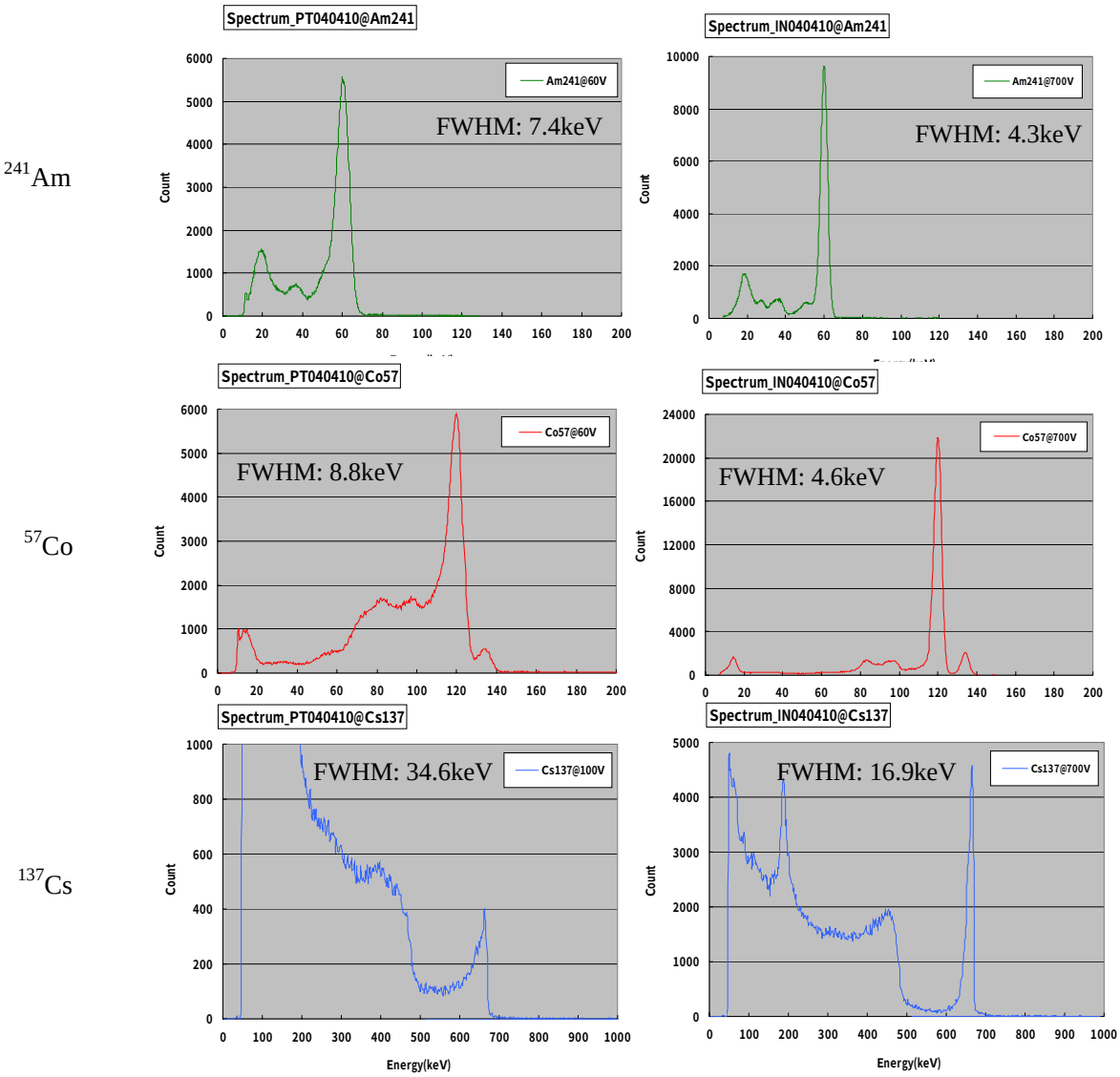

Fig.7 Energy spectra of the “Ohmic detector”(left) and “Schottky detector”(right)

The energy resolution of the "Ohmic detector" is not so good as that of "Schottky detector", however, it shows the very good time stability. Fig.8 shows the ^{241}Am spectra over 24 hours under the continuous bias application. The detector size was 4x4x1mm^3 and the bias voltage was 60V. The spectra are completely overlapped, showing the good stability. The "Ohmic detector" can be used very easily due to the stability and the low operation bias. European Space Agency has built-up the gamma telescope satellite "INTEGRAL" using about 16,000 pieces of the "Ohmic detector" and launched in 2002 [14].

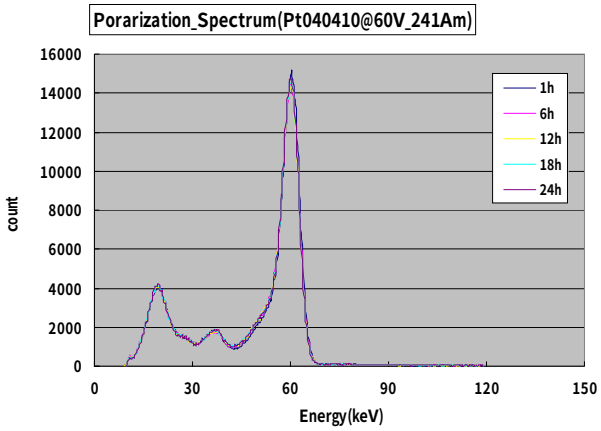

Fig.8 Evolution of the energy spectra of the "Ohmic detector"

Fig.9 shows the evolution of the energy spectra of the "Schottky detector" after bias applied. The detector size was also 4x4x1mm^3 and bias voltage was 700V. The very small change in the peak height could be seen in the spectra until 60 min after the bias applied, then the severe degradation occurred. This phenomenon is so called "polarization".

The effect of the bias voltage on the polarization is shown in Fig.10. In case of 300V, the FWHM starts increasing soon after the bias is applied and the peak channel decreasing at the same time. However, by increasing the bias voltage, the stable period of the FWHM and the peak channel appears and gets longer.

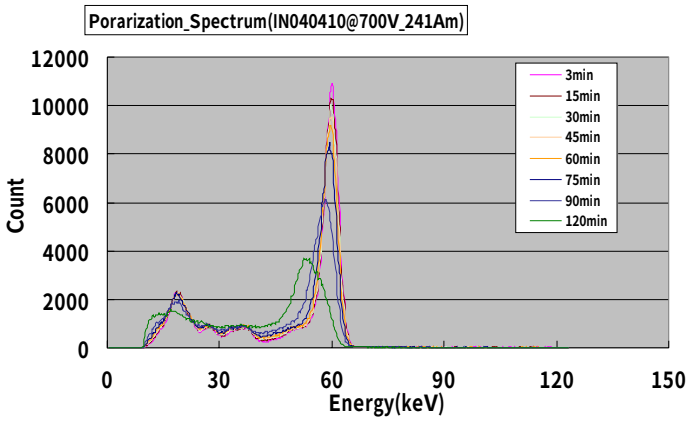

Fig.9 Evolution of the energy spectra of the "Schottky detector"

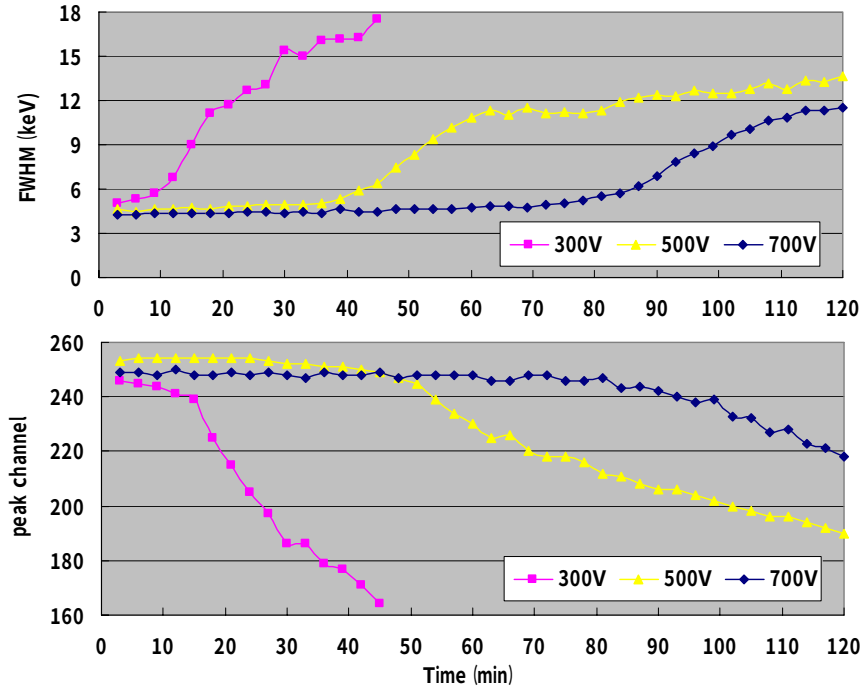

Fig.10 The effect of the bias voltage on the polarization. The upper and lower graphs are the photo-peak's FWHM and peak channel, respectively.

The effect of the detector thickness and the bias voltage on the polarization is shown in Fig.11. The bias voltage is normalized by the thickness of the detector. Apparently, the thinner detector at higher bias voltage is more stable at the same normalized bias (~electric field), and the 0.5mm thick detector is stable for 5hours at 600V/mm.

For any applications, the severe degradation of the spectrum must be avoided so that the detector is required to be recovered from the polarization. Fig.12 shows the recovery from the polarization by interrupting the bias voltage. The energy spectra of 3min, 30min and 60min after the bias application were measured, and the bias unit was turned off for one second and turned on to measure the spectra again. The spectra before and after the bias off were plotted with solid lines and cross markers, respectively. During the stable period (3min and 30min), the spectra before and after the bias-off were well overlapped, showing the detector was recovered from the polarization by the bias-off. As a result, the Schottky detector can be used for a long time by interrupting the bias periodically during the stable period.

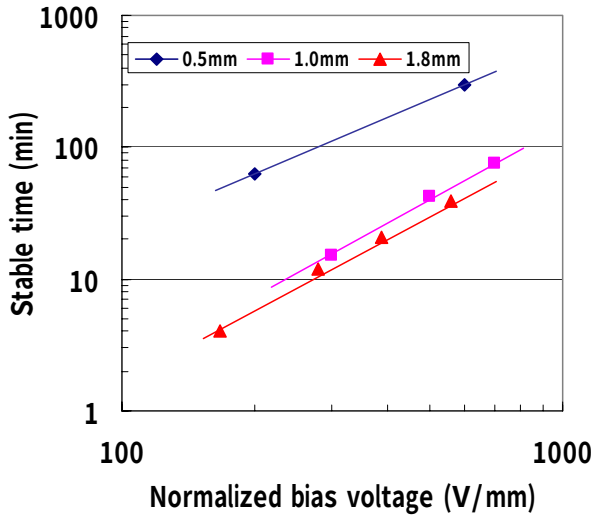

Fig.11 The effect of bias voltage and the detector thickness on the polarization

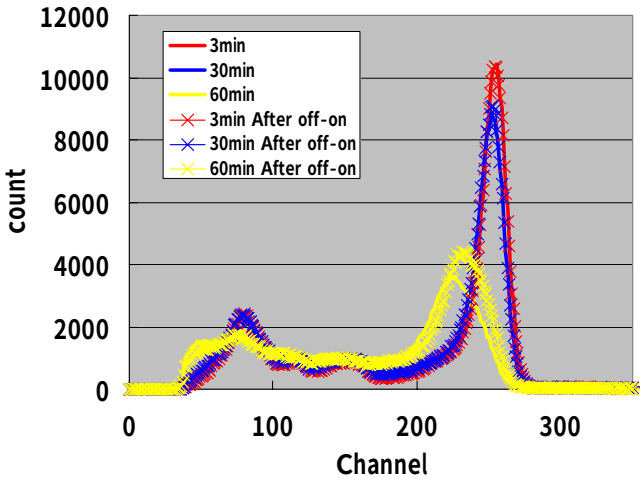

Fig.12 The recovery from the polarization by interrupting the bias. After the bias turned off for a second, the spectra are plotted by cross markers

The uniformity of the grown crystal is shown in Fig.13. 8959 pieces of the Schottky detector (5.5x5.5x1mm^3) were fabricated from one whole crystal ingot of 75mm diameter. The average FWHM and the standard deviation for the 662keV photo-peak were 12.9 keV and 3.4 keV, respectively. About 95% of the detectors have the resolution of better than 20keV (~3%), showing that the whole crystal ingot has the enough quality to fabricate the detector for the many applications.

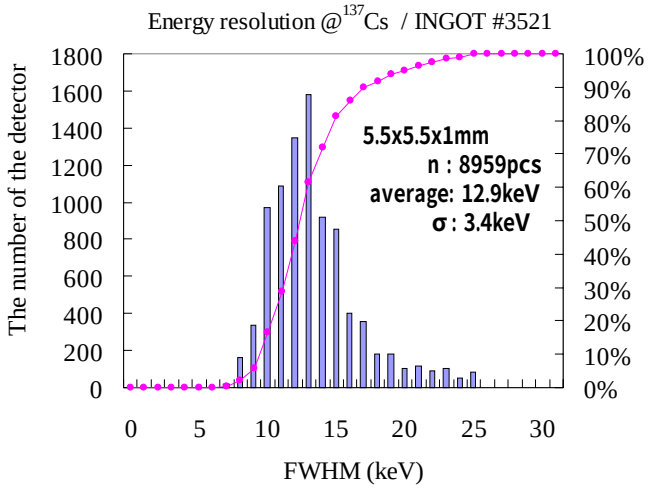

Fig.13 The histogram of the energy resolution at 662keV

4. Medical applications of the CdTe detector

Among the various applications, the medical field is probably the largest market for the CdTe detector. The examples of the medical application using the X-ray and gamma ray are shown.

Recently, Finish company Oy AJAT Ltd. has developed the x-ray imaging sensors using the CdTe pixellated detector and the C-MOS read-out ASIC. An application is the dental panorama camera, taking advantage of the high sensitivity, high resolution and high contrast. Fig.14 shows the structure of the CdTe imaging sensor. The CdTe pixellated detector is connected to the C-MOS read-out ASIC by Flip-Chip bonding. The charge induced by the x-ray is measured at the each pixel on the ASIC. In this application, the scintillator-CCD flat-panel is also used and the comparison of both imagers' principle is shown in Fig.15. In case of the scintillator-CCD system, the x-ray is converted into the light emission in the scintillator, which is detected by the CCD. As the emission of the light occurs non-directionally, not only the CCD pixels under the irradiated area but also pixels around the area can detect the signal and the image is blurred. On the other hand, the CdTe detector converts the x-ray radiation into the electric charge, which is straightforwardly pulled along the line of the electric force. Therefore, only the pixel right under the irradiated area can detect the signal and the clear image can be constructed.

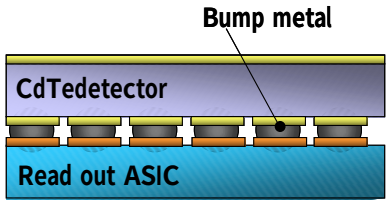

Fig.14 The structure of CdTe imaging sensor for the dental panorama camera

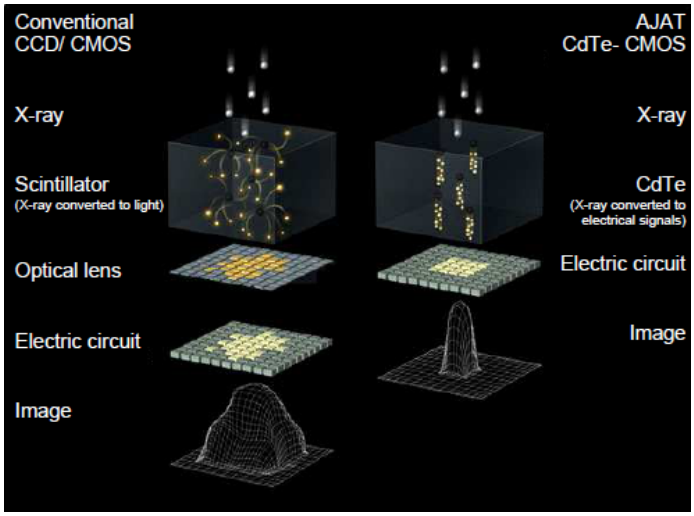

Fig. 15 The difference between the Scintillator –CCD and the CdTe-CMOS

The dental panorama images taken by the scintillator / CCD sensor and the CdTe / C-MOS sensor are shown in Fig. 16. The sharper outline and the better contrast could be obtained by the CdTe/C-MOS sensor. This CdTe/C-MOS imaging sensor technology is thought to be applicable for the X-ray CT, X-ray mammography, etc. in medical field as well as non-destructive sensing, security applications.

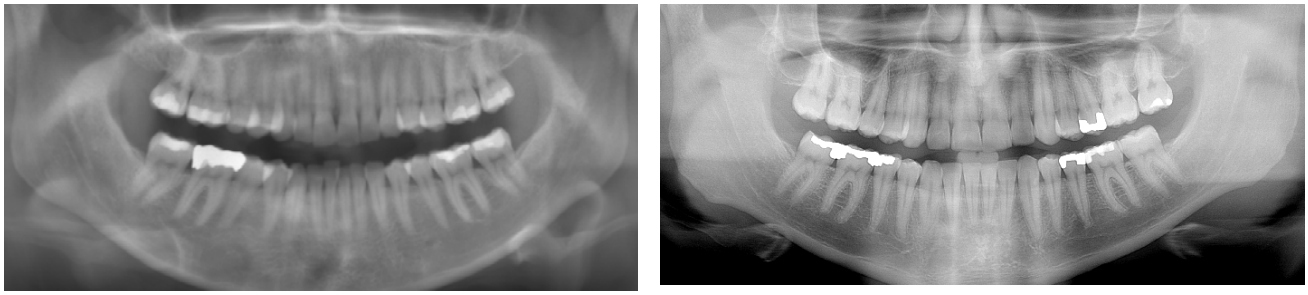

Fig.16 The images taken by the scintillator /CCD(left) and by the CdTe/C-MOS (right) (by courtesy of Oy AJAT Ltd.)

An example of the gamma ray imaging is shown in Fig. 17. This is a hand-held " Mini-Gamma-Camera (MGC-500) " developed by Acrorad. The 32 x 32 pixel CdTe 2-D array (1024ch, FOV 45x45mm) enables the energy resolution of better than 6% at 122 keV and the spatial resolution of 1.4 mm. Thanks to the high sensitivity and the spatial resolution, it is very useful device to find the sentinel lymph node during the cancer surgery [15,16]

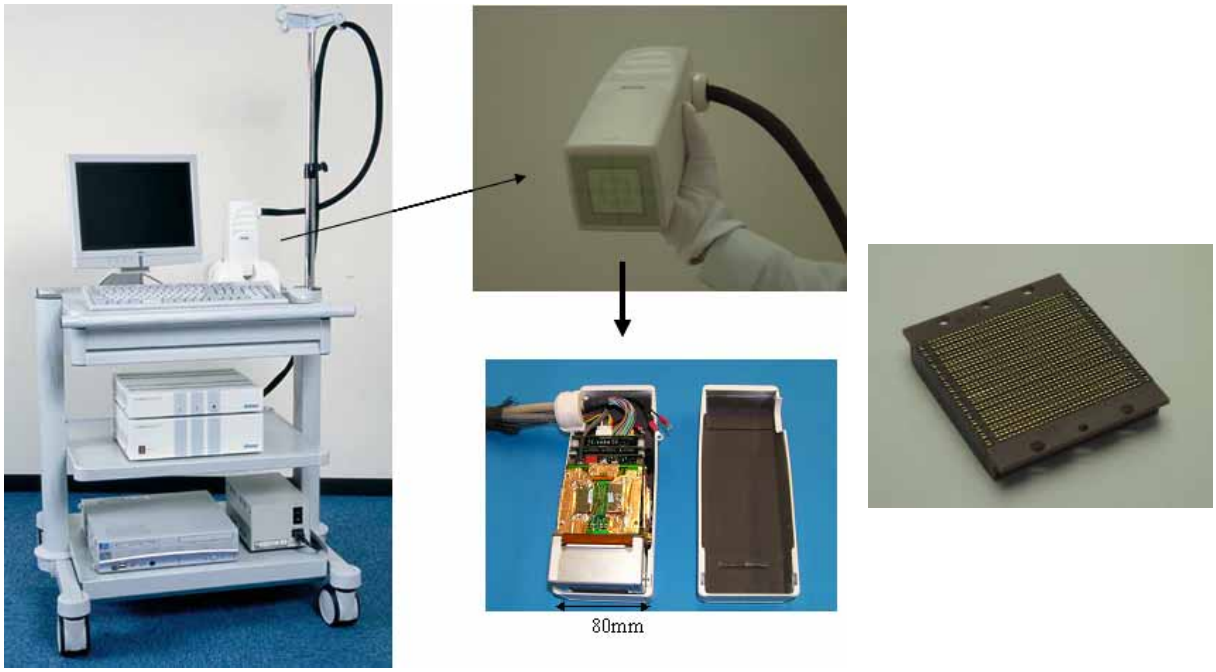

Fig.17 The whole system of Mini-Gamma-Camera (left) is portable and able to be used in surgery. The camera is of hand-held size (middle top) and contains the collimator, the CdTe detectors and the read-out ASICs (middle bottom). The 32x32 channel array of CdTe detector module (FOV 45x45mm) (right)

5. Conclusion

The intensive works for the development of CdTe detector have been carried out in Acrorad for almost 20 years and the results are summarized as follows;

(1) The CdTe single crystal of 75mm diameter has been able to be grown for the detector mass production.
(2) The "Ohmic detector" can be operated at relatively low bias voltage and shows the good time stability.
(3) The "Schottky detector" shows the superior energy resolution but it degrades with time (polarization). The thinner detector at higher bias voltage shows the longer stable period. The detector can be recovered from polarization by turning off the bias for one second.
(4) The whole crystal ingot is found to have the enough quality and uniformity to fabricate the detector for the many practical applications.
(5) The CdTe detector applications for X-ray and gamma ray imaging in the medical field are presented.

Acknowledgements

The authors wish to thank Dr. Konstantinos Spartiotis at Oy AJAT Ltd. for providing the data of dental panorama camera and the images.

References

[1] Kenneth Zanio, Journal of Electronic Materials, Vol.3, No.2, page327 (1973)
[2] R.Triboulet, Y.Marfaing, A.Cornet and P.Siffert, Journal of Applied Physics, Vol.45, No.6 (1974)
[3] F.V.Wald and G.Entine, Nuclear Instruments and Methods Vol.150, page13 (1978)
[4] Y.Iwase, H.Takamura, K.Urata and M.Ohmori, Sensors and Actuators A, Vol.34, page31 (1992)
[5] Y.Iwase, M.Funaki, A.Onozuka and M.Ohmori, Nuclear Instruments and Methods in Physics Research A, Vol.322 page628 (1992)
[6] Y.Iwase, R.Ohno and M.Ohmori, Material Research Society Symposium Proceedings, vol.302, page225 (1993)
[7] M.Ohmori, Y.Iwase ans R.Ohno, Materials Science and Engineering, Vol.B16, page283 (1993)

[8] T.Ozaki, Y.Iwase, H.Takamura and M.Ohmori, Nuclear Instruments and Methods in Physics research A, Vol.380, Page141 (1996)
[9] M.Funaki, T.Ozaki, K.Satoh and R.Ohno, Nuclear Instruments and Methods in Physics Research A, Vol.436 page120 (1999)
[10] M.Moriyama, M.Kunisu, A.Kiyamu, R.Ohno and M.Murakami, Materials Transactions, Vol.46, No.9, Page1991 (2005)
[11] T.E.Schlesinger and Ralph B. James, "Semiconductors for Room Temperature Nuclear Detector Applications", Semiconductor and semimetals vol.43, page221 (1995)
[12] C.Matsumoto, T.Takahashi, K.Takizawa, R.Ohno, T.Ozaki and K.Mori, IEEE Trans. Nucl.Sci., Vol.45, page428 (1998)
[13] T.Takahashi, B.Paul, K.Hirose, C.Matsumoto, R.Ohno, T.Ozaki, K.Mori and Y.Tomita, Nuclear Instruments and Methods in Physics A, Vol.436, page 111(1999)
[14] O.Limousin, A.Claret, E.Delagnes, P.Laurent, F.Lebrun, F.Lugiez, A.Sauvageon and R.Terrier, Nuclea Science Symposium Conference Record, 2003 IEEE Vol.5, page3555 (2003)
[15] M.Tsuchimochi, H.Sakahara, K.Hayama, M.Funaki, R.Ohno, T,Shirahata, T.Orskaug. G.Maehlum, K.Yoshioka, E.Nygard, Eur.J.Nucl.Med.Mol.Imaging, Vol.30, Page1605 (2003)
[16] C.Tanaka, H.Fujii, A.Shiotani, Y.Kitagawa, K.Nakamura and A.Kubo, Clin.Nucl.Med. Vol.30, page440 (2005)